https://doi.org/10.5194/acp-2021-876
Preprint. Discussion started: 20 November 2021

Atmospheric Chemistry and Physics Discussions

The impacts of marine-emitted halogens on OH radical in East Asia during summer

Shidong Fan[1,2], Ying Li[1,2]

[1]Department of Ocean Science and Engineering, Southern University of Science and Technology, Shenzhen 518055, China
[2]Center for the Oceanic and Atmospheric Science at SUSTech (COAST), Southern University of Science and Technology, Shenzhen 518055, China

Correspondence to: Ying Li (liy66@sustech.edu.cn)

Abstract. Relationships between oceanic emissions and air chemistry are intricate and still not fully understood. For regional air chemistry, a better understanding of marine halogen emission on Hydroxyl (OH) radical is crucial. OH radical is a key species in atmospheric chemistry because it can oxidize almost all trace species in the atmosphere. In the marine atmosphere, OH level could be significantly affected by the halogen species emitted from the ocean. However, due to the complicated interactions of halogens with OH through different pathways, it is not well understood how halogens influence OH and even what the sign of the net effect is. Therefore, in this study, we aim to quantify the impact of marine-emitted halogens (including Cl, Br, and I) through different pathways on OH in the high OH season by using WRF-CMAQ model with process analysis and state-of-the-art halogen chemistry in the East Asia Seas. Results show a very complicated response of OH production rate (P_{OH}) to marine halogen emissions. The monthly P_{OH} is generally decreased over the ocean by up to a maximum of about 10–15% in the Philippine Sea, but is increased in many nearshore areas by up to about 7–9% in the Bohai Sea. In the coastal areas of southern China, the monthly P_{OH} could also decrease 3–5% in the Greater Bay Area, but with a daytime hourly maximum decrease over 30%. Analysis of the individual reactions using integrated reaction rate (IRR) show that the net change of P_{OH} is controlled by the competitions of three main pathways through different halogen species. Sea spray aerosols (SSA) and inorganic iodine gases are the main species to influence the strengths of these three pathways and therefore have the most significant impacts on P_{OH}. Both of these two types of species decrease P_{OH} through physical processes, while generally increase P_{OH} through chemical processes. In the ocean atmosphere, the controlling species are inorganic iodine gases and the complicated iodine chemistry determines the basic pattern of ΔP_{OH}, while over the continent, SSA is the controlling species and the SSA extinction effect leads to the negative ΔP_{OH} in the southern China. Our results indicate that marine-emitted halogen species have notable impacts over the ocean and have potential impact on the coastal atmospheric oxidation. The identified main (previously known or unknown) pathways and their controlling factors from different halogen species to OH radical explains the halogen-induced change of P_{OH} in East Asia and also can be applied in other circumstances (e.g., different domains, regions, and emission rates).

https://doi.org/10.5194/acp-2021-876
Preprint. Discussion started: 20 November 2021

Atmospheric Chemistry and Physics Discussions

1 Introduction

Hydroxyl radical is the most important daytime oxidant in the troposphere. It can oxidize almost all directly emitted gases such as CO, CH_4 and other VOCs, while produce some secondary species such as O_3 and secondary aerosols at the same time. The dominant sources of OH are HO_2 and O_3 over the continental areas, through the reaction of HO_2 with NO and the photolysis of O_3 and following reaction of O^1D with water vapor, respectively. At urban areas, the photolysis of HONO is also a significant source of OH, and may be more important than the photolysis of O_3, especially in spring, autumn, and winter because of the very large seasonal variation of O_3 photolysis and humidity (e.g., Tan et al., 2019;Whalley et al., 2021;Liu et al., 2019). The main sinks of OH are CO and VOCs. Recently, studies showed that in the low-NO*x* conditions, OH modeled by current chemical mechanisms are usually underestimated (Tan et al., 2019;Rohrer et al., 2014;Lelieveld et al., 2008;Hofzumahaus et al., 2009;Lu et al., 2019a;Fuchs et al., 2013;Stone et al., 2012;Fittschen et al., 2019;Whalley et al., 2021), and missing sources of OH is a common hypothesis. To account for such a missing source of OH, efforts have been made to update RO_2 chemistry, by introducing artificial pathways first and mechanistic pathways later that convert RO_2 to OH (e.g., Bates and Jacob, 2019;Archibald et al., 2010). However, due to the complexity of RO_2 chemistry, current understanding on the missing source of OH in the low-NO*x* condition is still open.

In the marine atmosphere, the abundant marine-emitted halogen species have significant impact on OH. The marine-emitted halogen could make the tropospheric HO*x*-NO*x*-O_3-VOCs chemistry more complex. One relevant reaction is that XO (X=Cl, Br, and I) transform HO_2 to OH, as NO does in the high-NO*x* condition. As a consequence, previous box-model studies usually showed positive impacts of halogen chemistry on OH (Stone et al., 2018;Whalley et al., 2010). However, there is an opposite impact of halogens on OH as usually shown by chemical transport model (CTM) studies that halogen species will consume O_3 which in turn would reduce the production of OH (e.g., Sherwen et al., 2016;Stone et al., 2018). In box-model studies, long-term species such as O_3 are usually observation-constrained and cannot reflect the influence of halogens, probably resulting the difference between box models and CTMs (Stone et al., 2018). Therefore, special attention needs to be paid when using box models to quantify the complicated impacts of halogen species on the HO*x*-NO*x*-O_3-VOCs chemistry. In CTMs studies, the two pathways (i.e., enhanced HO_2 conversion by XO and O_3 consumption by X atoms) are well described, but it is not very clear which process will dominate. Furthermore, the impacts of halogen species on OH are actually more complex than the two pathways. First, there may be other important impacts of halogen on the sources or sinks of OH. For example, the conversion of HO_2 to OH enhanced by XO would consume HO_2, which in turn should decrease the conversion through HO_2+NO. Previous CTM studies generally did not consider such an impact (e.g., Stone et al., 2018). Besides, other sources of OH, including the photolysis of HONO and H_2O_2, ozonolysis of some alkene, and the decomposition of some fragmentation of the aromatic hydrocarbons, as well as the chemistry of peroxyl radicals could also be influenced by halogen chemistry. Second, different halogen species generally have different impacts on OH, indicating different controlling factors to the pathways for different halogen species, making the net impact of all halogen species variable. For example, Stone et al. (2018) showed iodine will generally increase OH while bromine the opposite, and their

https://doi.org/10.5194/acp-2021-876
Preprint. Discussion started: 20 November 2021


Atmospheric Chemistry and Physics Discussions

combined effect is more subtle. However, previous studies did not analyze the pathways themselves and it remains unclear what processes control the strengths of the known and unknown (if exist) pathways of different species and how these pathways interact. Moreover, since current estimations of marine halogen emissions have large uncertainties, the stability of the interaction result of different pathways may be subject to the uncertainties in the emission estimation and variation in controlling factors of the various pathways.

In short, recent studies in understanding the impacts of halogen chemistry on OH usually focused on the two pre-described pathways (i.e., enhanced HO_2 conversion by XO and O_3 consumption by X atoms) which are not directly quantified. Therefore, in order to better understand the role of halogen chemistry on tropospheric OH, we explore the pathways by which halogen species influence OH, and how these pathways interact with each other in this study, based on current knowledge about halogen chemistry and marine emissions of halogen species. We use process analysis (PA, including Integrated Process Rate, IPR, and Integrated Reaction Rate, IRR) in a CTM (CMAQ) to separate different pathways. Furthermore, the controlling factors of strengths of the different pathways are analyzed based on PA and relevant sensitivity simulations, and their interactions are discussed. The emission uncertainties are taken into consideration by running sensitivity simulations using extreme emission rates that have been used in previous studies. The setup of the models and the estimations of marine emission and its extreme uncertainties of halogen species are described in Section 2. Results and discussions are in Section 3. Section 4 gives conclusions.

2. Methods

2.1 Model setup

We use the CMAQ model, driven by meteorological fields from WRF, to explore the impact of halogens on OH. For WRF (version 3.9.1), the domain has a horizontal resolution of 27km and the number of grids is 283×184. The vertical coordinates contain 39 sigma levels. The initial and boundary conditions are generated from the NCEP GDAS/FNL 0.25° analysis data. Analysis and observation nudging are applied. The data used for observation nudging are obtained from NCEP datasets *ds461.0* (for surface) and *ds361.1* (for upper layer). For major physical parameterizations, the Rapid Radiative Transfer Model (RRTM) longwave radiation scheme, the Dudhia shortwave radiation scheme, the WRF Single-Moment 3-class microphysics scheme, the Noah Land Surface Model, and the Grell-Freitas ensemble cumulus scheme are applied.

CMAQ (version 5.3.2) (Appel et al., 2021) has the same horizontal resolution as WRF, but with a slightly smaller domain. The vertical layers are the lowest 20 layers plus six of the remaining 19 layers of WRF. The chemical mechanisms adopted here is CB6r3m released in CMAQv5.3. Rosenbrock (ROS3) solver is used to solve the chemical reactions and the absolute and relative error tolerances are set to 10^{-9} ppm and 10^{-3}, respectively. The initial and boundary conditions for CMAQ are extracted from a seasonal average hemispheric CMAQ output file that is obtained from the CMAS data warehouse (https://github.com/USEPA/CMAQ/blob/master/DOCS/Users_Guide/Tutorials/CMAQ_UG_tutorial_HCMAQ_IC_BC.md, last access: 6 October 2021). This hemispheric CMAQ used the same chemical mechanism as ours. The anthropogenic

https://doi.org/10.5194/acp-2021-876
Preprint. Discussion started: 20 November 2021


Atmospheric Chemistry and Physics Discussions

emissions are from MEIC (http://www. meicmodel.org/), while the emissions in the Guangdong province are replaced by local emissions that are based on a local emission inventory (Yin et al., 2015;Zheng et al., 2009) and processed by the Sparse Matrix Operator Kernel Emissions (SMOKE) processor. No halogen species are contained in the anthropogenic emissions. The terrestrial biogenic emissions are processed by MEGAN2.1 (Guenther et al., 2012).

Because OH concentration is highest in summer, the simulations of this study are for the month of July 2019, including an additional 10 day in June for spin-up following Li et al. (2020).

2.2 Marine emissions of halogen species

There are three main types of halogen species emitted from the ocean: SSA (Cl and Br), inorganic iodine (I_2 and HOI), and halocarbons including $CHBr_3$, CH_2Br_2, CH_2BrCl, $CHBr_2Cl$, $CHBrCl_2$, CH_3I, CH_2ICl, CH_2IBr, and CH_2I_2 (e.g., Sarwar et al., 2019;Carpenter et al., 2013;Ordonez et al., 2012;Wang et al., 2019). The latest release version of CMAQ (v5.3) contains these emissions inline.

The SSA emission in current CMAQ is updated by Gantt et al. (2015) on the top of the work of Kelly et al. (2010). The source function is based on the widely used source function developed by Gong (2003) which is an update of Monahan et al. (1986). Two main changes were implemented by Gantt et al. (2015). One is to add an SST-correction function to the source function because SST has large impacts on SSA flux (e.g., Barthel et al., 2019;Liu et al., 2021). The other is to change the shape factor of the source function (which determines the shape of the flux distribution) to emit more submicron SSA (see Fig. S1 of Gantt et al. (2015)). The SST-correction function is based on the work of Ovadnevaite et al. (2014) and is linear. This is different from another widely used observation-based SST-correction function developed by Jaeglé et al. (2011) which is a 3-order function of SST, but at high temperature (~30°C) their values are close (see Fig. S3 of the preprint version of Ovadnevaite et al. (2014)). Besides these two main changes, surf-enhanced emission is also reduced by narrowing the surf zone which was previously defined as 50 m to the coast and now reduced to 25 m as in the study of Gantt et al. (2015).

Inorganic iodine and halocarbons, as well as Br in SSA, are implemented as by Sarwar and co-workers (Sarwar et al., 2019). Inorganic iodine emissions are based on the work of Carpenter et al. (2013) which parameterized the emission of I_2 and HOI as functions of O_3 concentration, aqueous iodine concentration, and surface wind speed (see eqs. 19 and 20 in the SI of Carpenter et al. (2013)). Halocarbon emissions are calculated based on the work of Ordonez et al. (2012) which directly related flux of halocarbons to chlorophyll-*a* (chl-*a*) concentration.

Current estimations of marine halogen emissions have large uncertainties. There are many different source functions of SSA, and the difference of the SSA flux calculated based on these source functions are very large (Grythe et al., 2014). The parameterizations of aqueous iodine have also different versions and differ largely (MacDonald et al., 2014;Sherwen et al., 2019;Chance et al., 2014). The halocarbon emissions are entirely empirical which have few physical bases. Therefore, it is necessary to consider the influence of the uncertainty in the emissions on final results. We design two simulation groups with different emission rates, one high and one low. The high and low emission rates are taken from previously used estimations, similar to the work of Sekiya et al. (2020). The low emission rate of SSA is calculated using the source function in Gong

https://doi.org/10.5194/acp-2021-876
Preprint. Discussion started: 20 November 2021


Atmospheric Chemistry and Physics Discussions

(2003) directly, while the high emission rate using the source function modified by Gantt et al. (2015) because adding SST-correction function is somewhat more important than using different source functions (Barthel et al., 2019) and the source function of Gong (2003) or its modifications are the most widely used one. The parameterizations of I_2 and HOI emissions are less variable and only that by Carpenter et al. (2013) is widely used. However, there are two widely used parameterizations of aqueous iodine with large difference. Therefore, the low emission rate of I_2 and HOI is calculated using low concentration of aqueous iodine, taking from MacDonald et al. (2014), while the high emission rate using high concentration, taking from Chance et al. (2014). The calculation of halocarbon emissions are constrained by global annual flux (Sarwar et al., 2015); therefore, we increase or decrease halocarbon emissions based on the ratios of global annual halocarbon fluxes reported by WMO (Engel et al., 2019) to that in Ordonez et al. (2012). The chl-*a* data are obtained from the merged products of the GlobColour data set (http://globcolour.info, last access: 6 October 2021) that is developed, validated, and distributed by ACRI-ST, France.

The emissions of inorganic iodine are accompanied by the consumption of O_3 at the ocean surface, but current CTMs do not couple these two processes. Instead, an enhanced O_3 dry deposition by oceanic iodine is usually added (Luhar et al., 2018;Fairall et al., 2007;Luhar et al., 2017). In CMAQ, this O_3 deposition to ocean is based on the work of Chang et al. (2004), and uses the oceanic iodine concentration parametrization by MacDonald et al. (2014) (Sarwar et al., 2015). We use the aqueous iodine parameterizations consistent with that in the calculation of inorganic iodine emissions above.

To investigate the contribution from different species and pathways, we in total carried out more than eight simulation runs other than the control run (BASE) in this study. The description of all the simulations and their differences are described in Table 1.

Table 1. Case design in this study.

Simulation case	Species	Emission rate and ref
BASE	--	--
All_high	SSA	High, from Gantt et al. (2015), ≈ Gong (2003) with SST correction from Ovadnevaite et al. (2014)
	I_2 and HOI	High, Carpenter et al. (2013) parameterization and Chance et al. (2014) aqueous iodine
	halocarbons	High, Ordonez et al. (2012) parameterization and enhancement based on Engel et al. (2019)
All_low	SSA	Low, Gong (2003)

https://doi.org/10.5194/acp-2021-876
Preprint. Discussion started: 20 November 2021

Atmospheric Chemistry and Physics Discussions

	I_2 and HOI	Low, Carpenter et al. (2013) parameterization and MacDonald et al. (2014) aqueous iodine
	halocarbons	Low, Ordonez et al. (2012) parameterization and diminution based on Engel et al. (2019)
SSA (SSA_Cl+Br)	Only SSA	As in All_high
SSA_Cl	As SSA but excluding Br	As in All_high
SSA_phy	As SSA_Cl but excluding[1] the activation reaction N_2O_5(g)+Cl(s)	As in All_high
SSA_chemCl	SSA_Cl−SSA_phy	--
SSA_chemBr	SSA−SSA_Cl	--
InorgI	Only I_2 and HOI	As in All_high
InorgI_chem	As InorgI but excluding enhanced O_3 dry deposition	Chang et al. (2004) & Sarwar et al. (2015)
O3depo	InorgI−InorgI_chem	--
HaloC	Only halocarbons	As in All_high

[1] The reaction is unchanged but the uptake coefficient of N_2O_5(g) and the yield of $ClNO_2$ are set to 0.

3. Results and discussions

3.1 Performance of the model

To evaluate the performance of our models, O_3, the key species for OH primary production, is compared between simulated and observed data over land (in China). The metrics for evaluation include the average observation (Obs_mean) and simulation (Sim_mean) values, root mean square error (RMSE), normalized mean bias (NMB), normalized mean error (NME), correlation coefficient (*r*), and index of agreement (IOA). The benchmarks are taken from the study of Emery et al. (2017). The statistical metrics of all stations is calculated and the average values are presented in Table 2. We evaluate stations in the three major polluted areas near the seas in mainland China, namely, the North China Plain (NCP), the Yangtze River Delta (YRD), and the Pearl River Delta (PRD) (Fig. S1). It can be seen that the O_3 concentrations are generally well simulated. Almost of these values meet the benchmarks.

Table 2. Model performance metrics for 1-hr O_3 in mainland China.

https://doi.org/10.5194/acp-2021-876
Preprint. Discussion started: 20 November 2021

Atmospheric Chemistry and Physics Discussions

Region	Obs_mean ($\mu g/m^3$)	Sim_mean ($\mu g/m^3$)	RMSE ($\mu g/m^3$)	NMB	NME	*r*	IOA
NCP	157.84	166.95	47.11	0.06 (< ±0.15)	0.24 (< 0.25)	0.61 (> 0.5)	0.75
YRD	134.46	154.48	52.56	0.15 (< ±0.15)	**0.31** (< 0.25)	0.59 (> 0.5)	0.71
PRD	132.93	141.79	41.48	0. 06 (< ±0.15)	0.23 (< 0.25)	0.74 (> 0.5)	0.83
Whole region	125.13	140.44	38.20	0.13	0.25	0.57	0.70

For the relevant halogen species, though the in-situ observational data over the marine area is limited, the model skills of marine halogens could generally be evaluated by the levels of BrO and IO due to their importance in halogen chemistry and the availability of the ship- and aircraft-based data and satellite remote sensing data (Li et al., 2020;Stone et al., 2018;Saiz-Lopez and von Glasow, 2012). Observations of BrO and IO very rare around the world, especially in East Asia Seas. In a cruise from Japan to Australia, Grossmann et al. (2013) measured IO, showing that IO concentration ranges from 1 to 2.2 pptv, with a typical daytime value ~1 pptv. The available measurements of mean concentrations of BrO in Western Pacific show 1.0, 1.7 and <0.5 pptv in three flights (Koenig et al., 2017) and 0.69 pptv (Le Breton et al., 2017) during two related campaigns (CONTRAST and CAST). These values are generally smaller than measurements in the Atlantic Ocean (e.g., Read et al., 2008). In addition, according to the global model results (Zhu et al., 2019) and satellite remote sensing (e.g., http://www.doas-bremen.de/bro_from_gome.htm, last access: 4 June 2021), surface BrO concentrations have large annual variations in the Western Pacific, with largest values in January while smallest values in July.

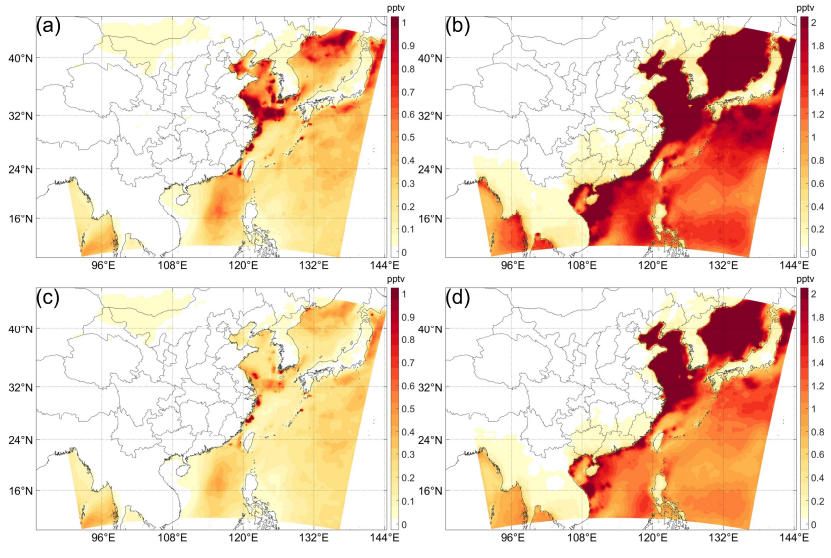

Figure 1. Daytime (local time 8:00–16:00) average of (a) BrO and (b) IO for high emission rate. (c) and (d) are for low emission rate.

https://doi.org/10.5194/acp-2021-876
Preprint. Discussion started: 20 November 2021

Atmospheric Chemistry and Physics Discussions

175

Table 3. Comparison of BrO and IO in the Philippine Sea in our simulations with observations and simulations reported in other studies.

	Mean/max				Platform
	Simulation, low emission rate	Simulation, high emission rate	Observation or model		
BrO	0.2/0.9 Jul	0.25/1.2 Jul	~1/2.9[a,1] Jan & Feb		Flights around Guam
			0.69/1.71[2] Jan		
			~1/>2[3] Jan	~0.3/>0.6[3] Jul	GEOS-Chem
IO	1.0/1.8 Jul	1.4/2.5 Jul	~1/2.2[4] Oct		Cruise from Japan to Australia

[a] only data at altitudes below 500 m.

[1] Koenig et al. (2017), [2] Le Breton et al. (2017), [3] Zhu et al. (2019), [4] Grossmann et al. (2013).

180 Figure 1 shows the daytime (local time 8:00-16:00) average BrO and IO simulated in our studies. Due to the lack of observation data in the coastal seas for comparison, we only discuss the results in the Philippine Sea (i.e., the open ocean east to the line connecting the Philippines, Taiwan, and Japan). In this sea, the concentrations of BrO and IO are generally lower than nearshore areas. The maximum mean values of daytime BrO and IO are 1.2 (0.9) and 2.5 (1.8) for high (low) emissions; for average over all these grids, the daytime BrO is about 0.25 (0.2) pptv, while IO about 1.4 (1.0) pptv for high
185 (low) emission rates.

Table 3 lists the comparison of the available measurements and global model results in the area and our model results. It can be seen that our model results generally agree well with measurements and other model results. It should be emphasized that the comparison is only indirect and there is a lack of data for even indirect comparison in the nearshore areas where the IO concentration is the largest. Since the inorganic iodine emission is closely related to O_3 concentration which is high in the
190 nearshore areas due to the outflow from the continent, the higher concentration of IO is reasonable, and in other regions, observations also support a very high concentration of IO in nearshore areas (Saiz-Lopez and von Glasow, 2012), but nevertheless, relevant observations are expected for a better validation.

https://doi.org/10.5194/acp-2021-876
Preprint. Discussion started: 20 November 2021


Atmospheric Chemistry and Physics Discussions

3.2 The changes of OH production rate (P_{OH}) and concentration

Figure 2 illustrates the halogen-induced changes of P_{OH} and OH concentration in All_high (all halogen species high emission rates) and All_low (all halogen species low emission rates) cases. ΔP_{OH} and ΔOH with both high and low emission rates all have similar spatial distributions but with different magnitudes. The most significant changes of P_{OH} and OH appear in the marine atmosphere (Fig. 2). The impacts are very complicated, with negative ΔP_{OH} and ΔOH in the middle area of the ocean while positive in the north and south parts of the ocean in the domain, but the area with negative impacts is larger than that with positive impacts. The decreases of OH can reach ~13% and ~8% (ΔP_{OH} ~15% and ~10%) in the Philippine Sea and the increase can reach ~11% and ~9% (ΔP_{OH} ~9% and ~7%) in the Bohai Sea, with high and low emission rate, respectively. This is in line with previous studies that generally showed decrease of globally-averaged OH but certain increase in some regions due to halogen chemistry (e.g., Sherwen et al., 2016;Stone et al., 2018;Wang et al., 2021). More specifically, in the East Asia seas, the studies of Stone et al. (2018), Wang et al. (2019) and Sherwen et al. (2016) generally showed slight decrease (<~5%) of annual-averaged surface OH while Stone et al. (2018) also showed slight increase in some regions. For studies in July, the study of Li et al. (2019) showed decrease of monthly averaged surface OH in the Atlantic Ocean near to Europe but increase in the Mediterranean Sea and the Baltic Sea. The decrease in the Atlantic Ocean can reach ~20% in the middle latitude. In the Indian Ocean, Mahajan et al. (2021) showed slight decrease (<5%) of monthly averaged surface OH near the Indian subcontinent while increase (<10%) near the equator, and the area with decreased OH is larger than that with increased OH in their model domain.

In the coastal areas the absolute changes of P_{OH} and OH can be comparable to or even larger than that over the ocean, but the relative values are relatively small due to the large absolute value over land (Figs. 2b, d, f, h). In the Greater Bay Area the decreases of monthly P_{OH} and OH are the largest, which can reach ~3–5% and ~4–6%, respectively (Figs. 2b,f).

Generally speaking, our results are comparable to previous studies, showing overall negative halogen-induced ΔOH but with complicated spatial distribution of negative and positive ΔOH (and ΔP_{OH}), especially in nearshore area. Previous studies have qualitatively and partially explained the reasons why halogens have such a complicated impact on OH, as the two pathways by which halogens influence OH (i.e., enhanced HO_2 conversion by XO and O_3 consumption by X atoms) have opposite impacts on OH (e.g., Stone et al., 2018). However, the complicated spatial distribution of negative and positive ΔOH indicates a complicated interaction of the pathways. Furthermore, it is unclear whether there are other important pathways by which halogens influence OH. Therefore, in order to better understand the impacts of halogens on OH, and more specifically, to understand why halogens increase OH in certain regions (especially nearshore area) but decrease in other regions, we need to find out all possible important pathways, and to further analyze the controlling factors of the strengths of the pathways.

In the following, we will further analyze the causes of such a complicated distribution. Since the spatial distributions of relative ΔP_{OH} and ΔOH are very similar despite the small difference in magnitudes, and the OH chemistry is generally discussed in terms of P_{OH} in literature (e.g., Tan et al., 2019;Hofzumahaus et al., 2009;Whalley et al., 2021) and we can

https://doi.org/10.5194/acp-2021-876
Preprint. Discussion started: 20 November 2021

Atmospheric Chemistry and Physics Discussions

directly separate different pathways by which influence P_{OH}, we will focus on P_{OH} in the following. Besides, because the patterns of ΔP_{OH} and ΔOH (Fig. 2), as well as the IRR results (Figs. 4 and S2), are quite similar in the All_high and All_low cases (Fig. 2), we will mainly focus on cases with high emission rates.

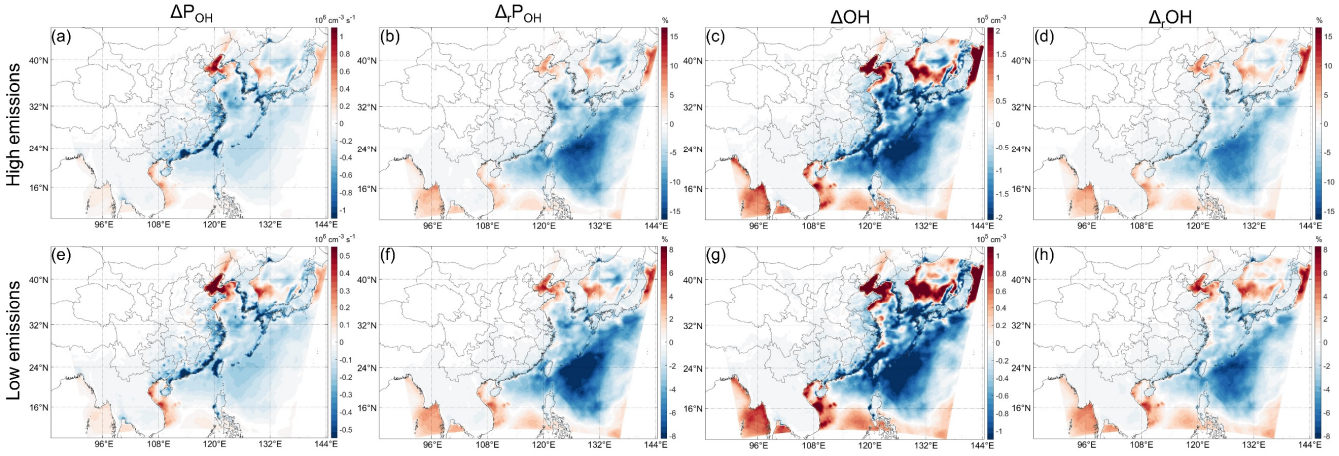

Figure 2. Change or relative change compared to BASE case of monthly averaged surface P_{OH} and OH in All_high case (first row) and All_low case (second row). The subscript "r" denotes "relative". Note the different scales in the All_high and All_low cases, the latter exactly a half to the former.

3.3 Quantification of different pathways' contributions

As mentioned above, there is complexity in the cause of the ΔP_{OH}. In this section, IRR is used to unravel important chemical reactions in changing P_{OH}. The main sources of OH in CB6 mechanism of CMAQ model include primary sources and secondary source. Primary sources include the photolysis of O_3, HONO, and H_2O_2, and ozonolysis of some alkenes. The secondary source is mainly the reactions HO_2+Y (Y=NO, O_3, etc.). With halogen chemistry, an additional primary source, HOX photolysis, needs to be considered. The changes of P_{OH} due to the change of these sources (denoted as ΔP_{OH_XX} in the following where XX is clear from the context) based on IRR analysis are illustrated in Fig. 3. It can be seen that the changes of photolysis of O_3 and HOX, and the reaction HO_2+Y are the main contributors to ΔP_{OH}. The photolysis of H_2O_2 changes small, while the other two sources almost remain unchanged. Other minor sources, including OH from RO_2, OH from FORM+O, as well as the photolysis of a hydroperoxyaldehyde from isoprene-derived RO_2 isomerization, contribute negligibly to ΔP_{OH}. We denote the halogen-induced change of these sources as pathways by which halogens influence OH and therefore there are three main pathways through which marine-emitted halogens influence P_{OH}, i.e., P_{OH_O1D}, P_{OH_HO2}, and P_{OH_HOX}.

In line with previous studies, the results show the change of O_3 and the addition of HOX are the two most important pathways by which halogens influence P_{OH} (Stone et al., 2018). ΔP_{OH} caused by the change of O_3 and HOX photolysis (denoted as ΔP_{OH_O1D} and ΔP_{OH_HOX} respectively) are very large in the north part of the ocean in the domain, especially in the Bohai sea and the Yellow sea, which is probably a result of the higher concentration of related species such as O_3 that is commonly reported at high concentration in the midlatitude in summer (e.g., Gao et al., 2020;Lu et al., 2019b;Hu et al.,

https://doi.org/10.5194/acp-2021-876
Preprint. Discussion started: 20 November 2021

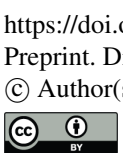

Atmospheric Chemistry and Physics Discussions

2017). ΔP_{OH_HOX} (Fig. 3f) can reach 4×10^6 cm^{-3} s^{-1} (~0.6 ppbv h^{-1}) for whole-day average and 1×10^7 cm^{-3} s^{-1} (~1.5 ppbv h^{-1}) for daytime average. Since HOX is a primary source of OH, and HO*x* budget studies generally ignored it (e.g., Tan et al., 2019;Hofzumahaus et al., 2009;Whalley et al., 2021), the large production rate of OH from HOX suggests the necessity to measure HOX in HO*x* budget studies under the potential influence of marine atmosphere.

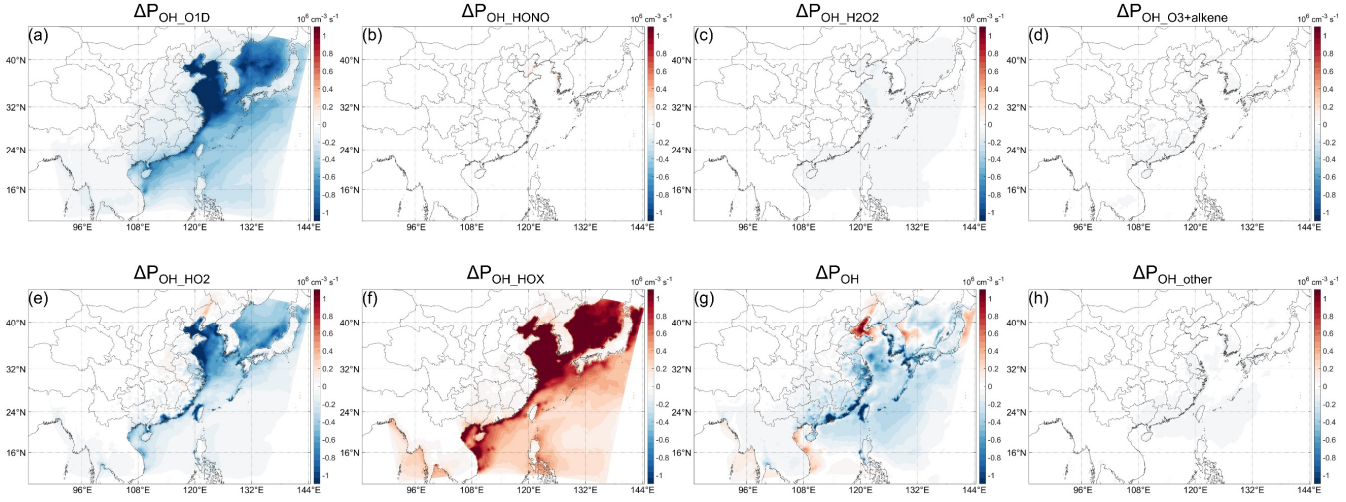

Figure 3. Change of P_{OH} (All_high–BASE case) caused by the changes of (a) O^1D (ΔP_{OH_O1D}), (b) HONO+hν (ΔP_{OH_HONO}), (c) H_2O_2+hν (ΔP_{OH_H2O2}), (d) O_3+alkene ($\Delta P_{OH\_O3+alkene}$), (e) HO_2+Y (ΔP_{OH_HO2}, Y=NO, O_3, etc.) and (f) HOX+hν (ΔP_{OH_HOX}). (g) is the net ΔP_{OH}, the same as Fig. 2a. (h) is the difference between ΔP_{OH} and the sum of (a)–(f).

In addition to ΔP_{OH_O1D} and ΔP_{OH_HOX}, ΔP_{OH_HO2} is also very important to ΔP_{OH} as shown in Fig. 3e. But, ΔP_{OH_HO2} was generally ignored in previous CTM studies, and box-model studies cannot accurately model the impact of the change of HO_2+Y on OH because NO and O_3 are observation-constrained (Stone et al., 2018;Whalley et al., 2010). The contribution of this pathway to the change of P_{OH} is significant. If we considered only ΔP_{OH_O1D} and ΔP_{OH_HOX}, only a relatively small area close to the Taiwan island would show negative ΔP_{OH} and the general impacts of halogens on OH would be positive (compare Figs. 3g and S3).

As mentioned above, the production rate of OH from HOX is very large. However, this large production rate is canceled by the large decrease of ΔP_{OH_O1D} and ΔP_{OH_HO2} (Figs. 3a,e), resulting the relatively small net ΔP_{OH} compared to ΔP_{OH_O1D} and ΔP_{OH_HOX} (and even ΔP_{OH_HO2} for many regions) over the ocean but still significant along the coastal areas (Fig. 3). It can be seen that the cancel-out effect of the three pathways with different signs result in the complicated spatial distribution of ΔP_{OH}, making ΔP_{OH} positive in the areas with larger ΔP_{OH_HOX} and negative otherwise. From these three pathways themselves, however, it is difficult to explain under what conditions ΔP_{OH_HOX} will be stronger than the other two pathways, and therefore difficult to explain why ΔP_{OH} is generally positive in the nearshore areas while negative in the open ocean. Then we need to further analyze the details of the processes influencing the strengths of these three pathways.

https://doi.org/10.5194/acp-2021-876
Preprint. Discussion started: 20 November 2021


Atmospheric Chemistry and Physics Discussions

3.4 Factors influencing the strengths of the three pathways

3.4.1 Overview of the contributions from different marine-emitted species

There are several factors that can change the strengths of the three main sources of OH (Fig. S4). Some of these factors are independent, some are interrelated. The independent factors include decrease of O_3 photolysis rate ($J(O^1D)$) and O_3 concentration by SSA-induced light extinction, and enhancement of O_3 deposition by oceanic iodine. The interrelated factors are generally closely related to halogen chemistry of which the most important reactions are the below three that for all three halogen elements and the fourth for Cl only (Saiz-Lopez and von Glasow, 2012;Simpson et al., 2015):

$$X + O_3 \rightarrow XO + O_2 \quad (R1)$$

$$XO + HO_2 \rightarrow HOX + O_2 \quad (R2)$$

$$HOX + h\nu \rightarrow X + OH \quad (R3)$$

$$Cl + VOCs \xrightarrow{O_2} RO_2 + HCl \quad (R4)$$

Since these factors are generally species-related, we separately modeled the impacts of different halogen species in addition to the case with all emissions (All_high) (Table 1). The results are shown in Fig. 4. It can be seen that the most significant contributors to the three pathways are inorganic iodine (Fig. 4e–g). However, the three pathways cancel out each other to a large extent and the resultant ΔP_{OH} is relatively small. Nevertheless, the impact of inorganic iodine is more positive than that of the all species together. The contribution of SSA to ΔP_{OH} is notable, comparable to that of inorganic iodine in most regions. There is positive contribution of SSA to ΔP_{OH} in the Bohai Sea and surroundings, while in other regions the contribution is negative. The negative contribution again neutralizes the positive contribution of inorganic iodine, resulting in a smaller ΔP_{OH} in All_high case (Fig. 3g) than in InorgI case (Fig. 4e). The contribution of halocarbons is relatively small and restricted to a small area near to the China coastline. Besides, the interactions between these three types of emitted species have very similar impacts with halocarbons but with opposing sign. Since we only focus on major contributions of different halogen species to ΔP_{OH}, we will not go into the details about the interactions of the three types of halogen emissions, and therefore we also do not discuss the influences of halocarbons in the following as they roughly cancel out the effects of the interactions. It should be noted, however, this does not imply that the interactions are caused by halocarbons.

https://doi.org/10.5194/acp-2021-876
Preprint. Discussion started: 20 November 2021

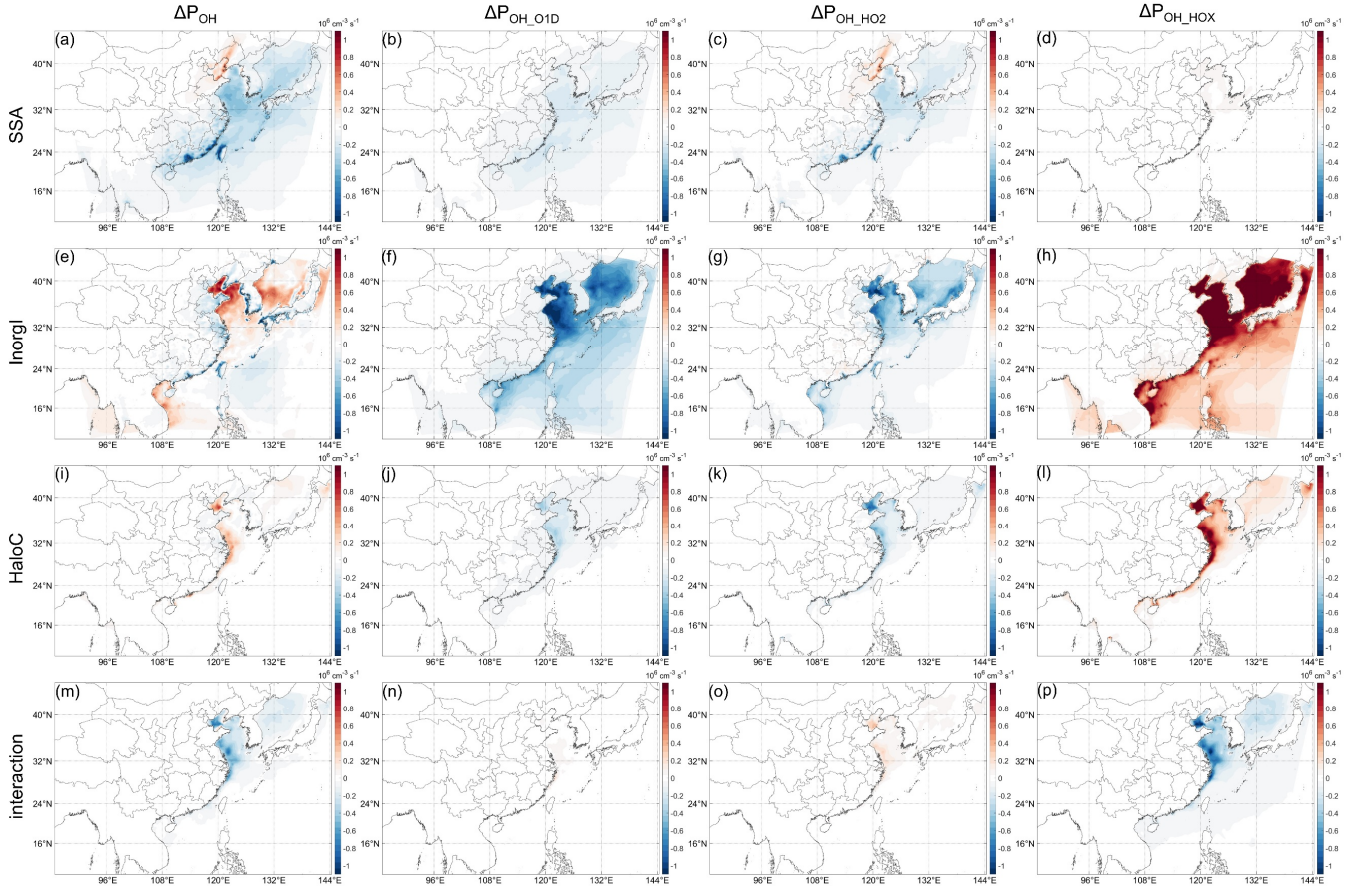

Figure 4. The changes of net OH production rate (ΔP_{OH}) and that induced by different pathways (ΔP_{OH_O1D}, ΔP_{OH_HO2}, and ΔP_{OH_HOX}) compared to BASE case. (a)–(d), (e)–(h), and (i)–(l) are results for SSA, InorgI, and HaloC case, respectively. (m)–(p) are the residue between All_high and SSA+InorgI+HaloC, representing the interactions of different halogen species.

3.4.2 Physical and chemical contributions of SSA emission

Regarding SSA, whose components are mainly Cl ions and inert non-volatile cations (NVCs, including Na, K, Ca, and Mg), with minor contribution from sulfate and Br ions, these emissions could influence OH through both actinic flux and chemical effects of Cl and Br (Fig. 5). The decrease of actinic flux caused by the extinction effect of SSA can decrease the photolysis rate constant of O_3 ($J(O^1D)$) and the O_3 concentration at the same time (Fig. S5), while the Cl and Br chemistry can increase or decrease O_3 and HO*x* radicals. Figure 5 indicates that the most important factor that determines the negative impact of SSA on P_{OH} (Fig. 4a) is its extinction effect. The negative impacts of Br chemistry are very small compared to this extinction effect. Besides the overall large impacts, the importance of the SSA extinction effect is also embodied in its impact on the continental atmosphere. As shown in Figs 4a,e,i the ΔP_{OH} over land induced by SSA is the most significant among the three halogen emissions, and here we know that the relatively large decrease of P_{OH} in southern China is caused by the extinction effect of SSA. In the Greater Bay Area the decrease of monthly P_{OH} caused by SSA can reach ~3% (with daytime maximum

https://doi.org/10.5194/acp-2021-876
Preprint. Discussion started: 20 November 2021

Atmospheric Chemistry and Physics Discussions

close to 30%). Therefore, even without halogen chemistry, adding SSA emissions in CTM studies may be important for atmospheric chemistry.

Another important factor that influences P_{OH} is the Cl chemistry (Fig. 5e–h). Similar to previous studies, Cl chemistry has positive impacts on ΔP_{OH} because Cl can oxidize VOCs efficiently and produce RO_2 radicals (Li et al., 2020;Wang et al., 2020;Simpson et al., 2015). Indeed, the change of P_{OH} by Cl chemistry is mostly through the change of OH production from HO_2 (Fig. 5f). The impacts of Cl chemistry are most significant in the Bohai Sea and surroundings. In these areas, the concentration of $ClNO_2$ (the key species for the activation of SSA Cl) and the Cl reactivity (k_{Cl}, $=\sum k_{Cl+VOC}\times[VOC]$) are higher than other regions (Fig. S6), resulting in the larger impact of the Cl chemistry. $ClNO_2$ is a product of N_2O_5 with particulate Cl, and N_2O_5 is a product of NO_2 and NO_3 radical (e.g., Yu et al., 2020). Therefore, the larger impacts of Cl chemistry in the Bohai Sea and surroundings probably reflect the influence of higher NO*x* and VOCs in the areas. The impact of Br chemistry on P_{OH} is quite small because it can merely influence O_3 concentration (Figs. 5i–l), and we will not discuss it further.

In regards to the three main pathways discussed in section 3.3, the physical contribution of SSA is achieved not only through the decrease of the photolysis of O_3 (both $J(O^1D)$ and the O_3 concentration) (Fig. 5b), but also through the decrease of HO_2 conversion to OH (Fig. 5c) which is probably feedback induced by the decrease of O_3 photolysis because HO_2 production is little influenced by photolysis change. In contrast, the chemical contribution of SSA Cl is achieved through the increase of RO_2, and therefore the second pathway, OH from HO_2, is more prominent (Fig. 5g), while the increase of O_3 concentration is of minor importance (Fig. 5f).

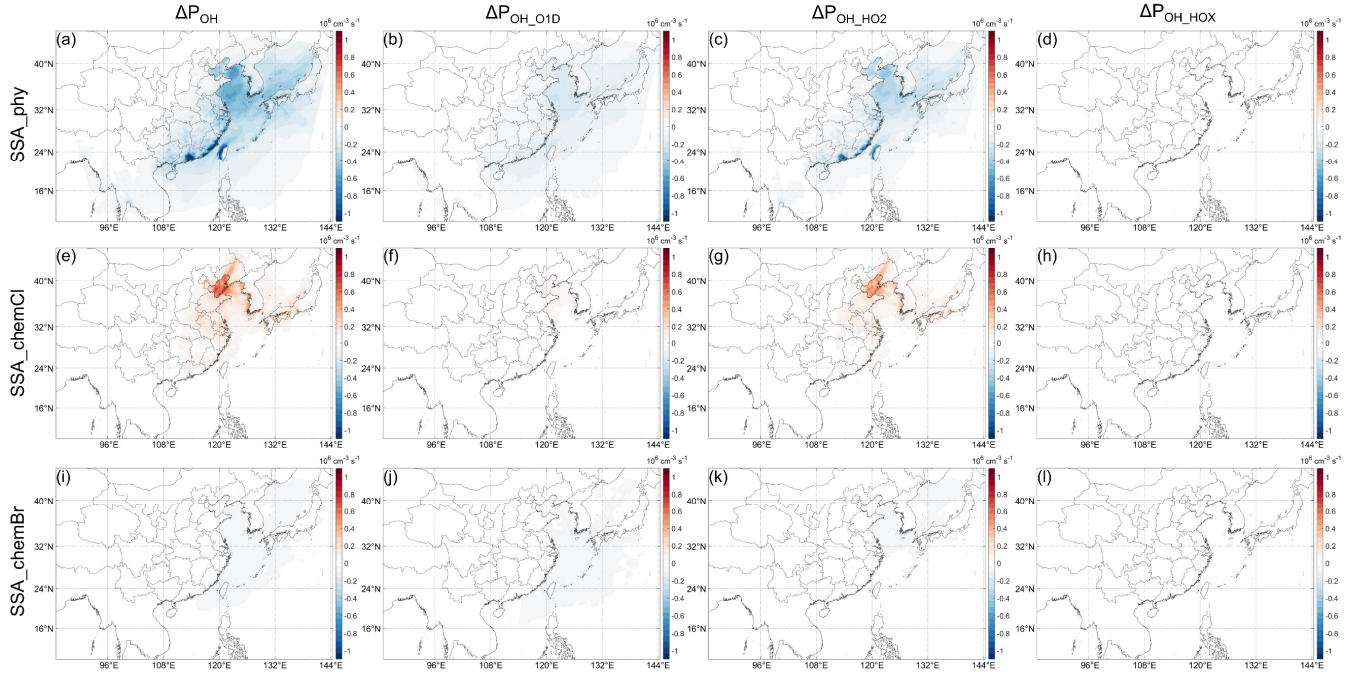

https://doi.org/10.5194/acp-2021-876
Preprint. Discussion started: 20 November 2021

Atmospheric Chemistry and Physics Discussions

Fig. 5. The changes of net OH production rate (ΔP_{OH}) and that induced by different pathways (ΔP_{OH_O1D}, ΔP_{OH_HO2}, and ΔP_{OH_HOX}) compared to BASE case, caused by (a)–(d) the extinction effect of SSA, denoted as SSA_phy, (e)–(h) Cl chemistry (only the activation of Cl through $ClNO_2$), and (i)–(l) Br chemistry.

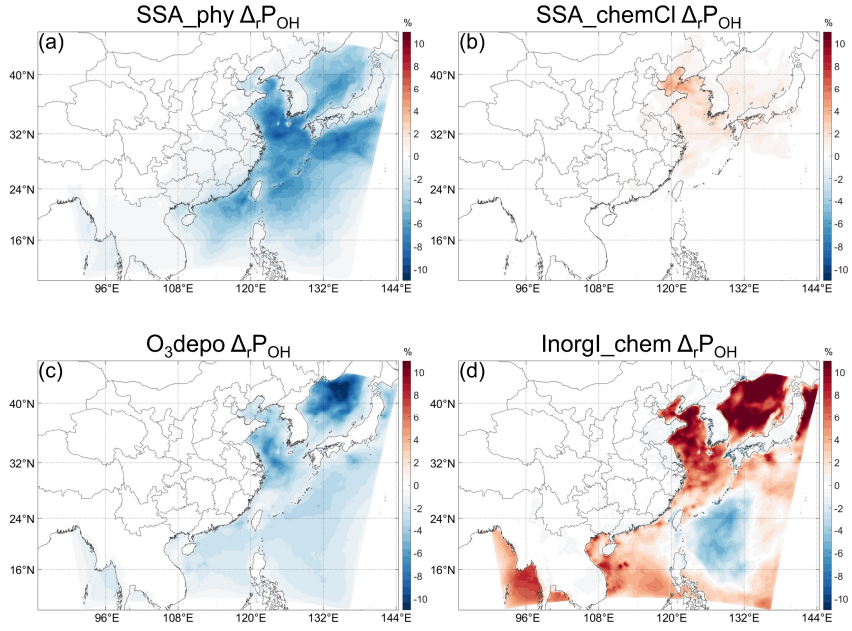

335 **Figure 6. Relative change of P_{OH} compared to BASE, caused by (a) SSA extinction effect, (b) SSA Cl chemistry, (c) enhanced O_3 deposition by aqueous iodine and (d) atmospheric inorganic iodine chemistry.**

3.4.3 Physical and chemical contributions of inorganic iodine species

Regarding the contributions from inorganic iodine species on ΔP_{OH}, the effects from the enhanced O_3 deposition by iodine ion in the ocean and atmospheric iodine chemistry (including the direct emission of HOI) should be considered. The change
340 of P_{OH} caused by the enhanced O_3 deposition is shown in Fig. 7a. The decrease of P_{OH} is most significant in the Bohai and Yellow Sea, where it can reach ~0.4×10^6 cm^{-3} s^{-1}, corresponding to ~6% (daytime hourly maximum > 30%) in the Yellow Sea relative to P_{OH} in the BASE case (Fig. 6c). The larger absolute decrease of P_{OH} is probably caused by the higher deposition of O_3 in the Bohai and Yellow Sea because of the higher O_3 concentration there as mentioned above. For the relative change, the decrease of P_{OH} is most significant in the Sea of Japan, where the relative decrease can reach more than
345 10% (daytime hourly maximum > 45%) (Fig. 6c). More specifically, this decrease of P_{OH} induced by O_3 deposition are caused by the decrease of O_3 (P_{OH_O1D}, Fig. 7b), and by the decrease of HOX photolysis (P_{OH_HOX}, Fig. 7d) which probably results from the slower cycling of HOI through reactions R1–R3 due to the lower O_3 concentration.

https://doi.org/10.5194/acp-2021-876
Preprint. Discussion started: 20 November 2021

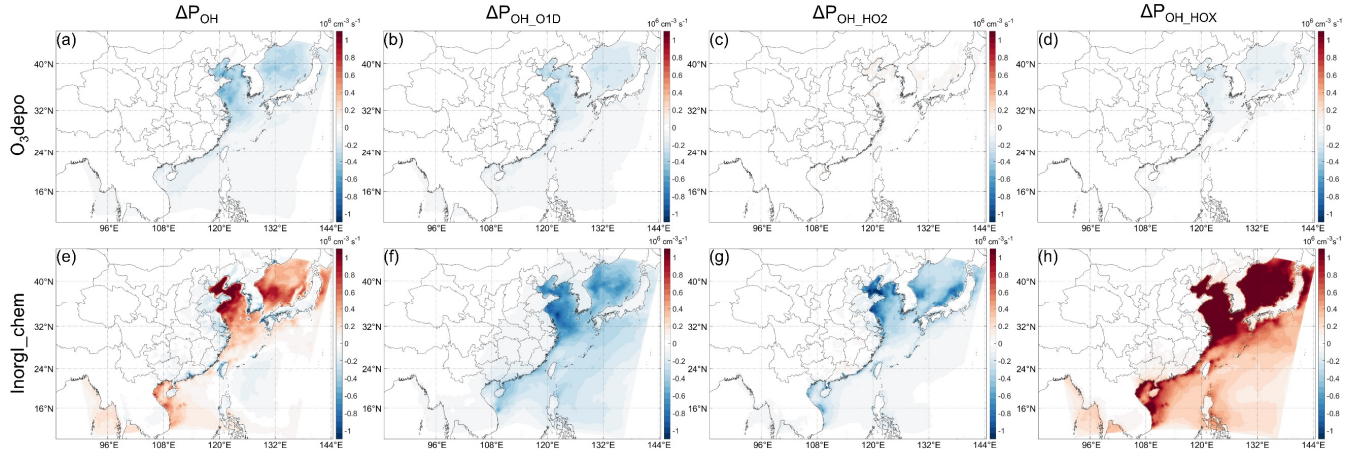

Figure 7. The changes of net OH production rate (ΔP_{OH}) and that induced by different pathways (ΔP_{OH_O1D}, ΔP_{OH_HO2}, and ΔP_{OH_HOX}) compared to BASE case, caused by (a)–(h) the enhanced O_3 deposition by oceanic iodine ions and (e)–(h) atmospheric iodine chemistry (including direct HOI emission).

Regarding the contributions from the atmospheric iodine chemistry on ΔP_{OH}, it has general positive impact on P_{OH} except in a limited areas in the Philippine Sea (Figs. 6d, 7e). The direct emission of HOI has only very small contribution (Fig. S7) and we will not discuss it further. The positive ΔP_{OH} in the Bohai and Yellow Sea can reach more than 1×10^6 cm^{-3} s^{-1} (~10% of BASE case) (Fig. 6d). In the Sea of Japan, the relative increase can reach more than 15%. It can be seen in Fig. 7 that the contributions of three pathways are all significantly influenced by iodine chemistry. Different from Cl chemistry, iodine chemistry can both increase P_{OH} via R3 (Fig. 7h) and decrease P_{OH} via R1–R2 (Figs. 7f–g). It is obvious that the competition between reactions R1/R2 and R3 can influence the net effect (positive or negative) of the iodine-chemistry-induced ΔP_{OH}. However, further analysis shows that the negative iodine-chemistry-induced ΔP_{OH} in the Philippine Sea is unlikely caused by the competition between O_3 loss rate and HOI cycling rate because these two rates are similar in the whole domain (Fig. S8c), but probably by the non-uniform response of O_3 concentration to the O_3 loss rate (Fig. S8e): O_3 concentration decreases more in the Philippine Sea than that is consumed by iodine there locally (see more details in SI). Compared to the physical net contribution of the inorganic iodine species, the net contribution of the iodine chemistry dominates the ΔP_{OH} pattern related to iodine shown in Fig. 4e.

3.4.4 Summary of the influences of the factors

In summary, we can conclude that the marine-emitted halogen species can result in a complicated change of P_{OH} in East Asia (Fig. 2), with negative ΔP_{OH} in the middle area of the ocean while positive in the north and south parts especially in the nearshore areas. IRR analysis results show that the changes of photolysis of O_3 and HOX, and the reaction HO_2+Y are the main contributors to ΔP_{OH} (Fig. 3). These three pathways are influenced by different factors related to different species. For the photolysis of O_3, both SSA and iodine can significantly decrease it, but with different mechanisms. SSA mainly influence the photolysis through a physical factor, by extinction solar radiation, which in turn can decrease both $J(O^1D)$ and

https://doi.org/10.5194/acp-2021-876
Preprint. Discussion started: 20 November 2021


Atmospheric Chemistry and Physics Discussions

O_3 concentration. Inorganic iodine can only decrease O_3 concentration, through the enhanced O_3 deposition and the atmospheric destruction of O_3, but to a much larger extent than that caused by SSA. For the photolysis of HOX, only the cycling of HOI has a significant contribution. For the conversion of HO_2 to OH, IO will compete with NO and O_3 to consume HO_2, resulting a significant decrease of the conversion; while the SSA can also lead to a decrease of the conversion, probably through more complicated feedbacks.

By influencing the strengths of the three pathways, these factors determine the pattern of the net ΔP_{OH}. More specifically, the basic pattern of ΔP_{OH}, with the largest relative decrease in the Philippine Sea (Fig. 2b), is controlled by the atmospheric iodine chemistry which shows negative ΔP_{OH} value only there (Fig. 6d), while the other marine areas can be roughly seen as the competition between the relatively evenly distributed negative ΔP_{OH} and the positive iodine-chemistry-induced ΔP_{OH}. In the Philippine Sea, the O_3 concentration decrease more than that is consumed locally, resulting in an "excessive" decrease of O_3 and therefore negative ΔP_{OH}. Other areas show more influence of local chemical consumption of O_3 (Fig. S8e), which is generally accompanied by the more efficient HOI cycling (and OH production) (Fig. S8c), and therefore positive iodine-chemistry-induced ΔP_{OH}. The HOI cycling is very strong in the northern seas (Fig. 7h), which is probably due to the higher levels of relevant gases such as O_3 that would result in high emission rates of inorganic iodine (Carpenter et al., 2013) and would enhance the cycling of reactions R1–R3.

In the Bohai Sea, the chemistry of SSA Cl also plays a role in increasing P_{OH}, probably due to the higher concentrations of NO*x* (for Cl activation) and VOCs (for RO_2 production) there. Similarly, the NCP also shows noticeable contribution of SSA Cl chemistry on ΔP_{OH}, but the impact is shaded by the negative contribution of SSA extinction effect on ΔP_{OH} (Figs. 4a, 5a,e).

3.5 Limitations

There are several limitations in our investigation. Our results rely much on the reliability of current halogen chemistry in CTMs, which is still under development. Recent model studies focused on the heterogeneous reactions of HOBr which can solve the problem of excessive BrO caused by debromination in GEOS-Chem (Wang et al., 2021;Zhu et al., 2019). But in our study, BrO is not excessive when including debromination and the contribution of Br chemistry to ΔP_{OH} is small, indicating the update of HOBr chemistry may not be critical to our results. The uncertainty in the Cl activation and its oxidations of VOCs may have larger impacts, but the recent update of N_2O_5 uptake in China does not improve Cl chemistry significantly (Dai et al., 2020), and due to the complexity of VOCs reactions, there are very few studies focused on the updates of Cl-VOCs chemistry. The largest limitation comes from the iodine chemistry because it is the main contributor to ΔP_{OH}. A recent observation study reported a much faster uptake of HOI and release of ICl and IBr (Tham et al., 2021), which may have large impacts on the cycling of HOI. Related to the iodine chemistry, the enhancement of O_3 deposition to the ocean is also not satisfactorily parameterized (Loades et al., 2020;Luhar et al., 2018;Pound et al., 2020). Therefore, the incomplete halogen chemistry may limit the representativeness of our results but probably result in a larger impact of halogen chemistry on OH.

https://doi.org/10.5194/acp-2021-876
Preprint. Discussion started: 20 November 2021


Atmospheric Chemistry and Physics Discussions

Another limitation is the absence of the uptake of HO_2 by aerosols in CMAQ. The emission of SSA will introduce a large number of particles into the atmosphere, which would obviously influence the uptake of HO_2. However, current knowledge about the uptake coefficient of HO_2 (γ_{HO2}) is rare and a constant 0.2 is generally used in CTMs (Song et al., 2020;Zhou et al., 2020;Zhou et al., 2021). With the lack of experiment- and/or observation-constrained parameterizations of the uptake of HO_2 by SSA, a constant γ_{HO2} and a large number of SSA particles may introduce large uncertainty in evaluating the impact on P_{OH} of SSA's uptake of HO_2. Therefore, we do not include the uptake of HO_2 in CMAQ (as default), but the limitation may be considered in further investigations when more are known about the HO_2 uptake.

4. Conclusions

To examine the mass interaction between ocean and atmosphere on the regional air oxidation capacity, we explore the impact of marine-emitted halogen species on atmospheric OH in East Asia in summer. The net ΔP_{OH} caused by all marine-emitted halogen species has both positive and negative signs in the marine atmosphere and the positive ΔP_{OH} appears mainly at nearshore areas. The monthly P_{OH} is generally decreased over the ocean with maxima of 10–15% in the Philippine Sea, but is increased in many nearshore areas, with maxima of 7–9% in the Bohai Sea. In the coastal areas of southern China, the monthly change of P_{OH} could also decrease 3–5% in the Greater Bay Area, but with a daytime hourly maximum decrease over 30%. These results indicate a notable impact of marine-emitted halogens on atmospheric oxidation capacity.

IRR analysis show that the net effect of ΔP_{OH} is controlled by the competitions of three main pathways through different halogen species, while the contributions of other pathways are minor. In additional to the two well-known pathways involving the changes of the photolysis of O_3 and HOX, the competition on HO_2 of XO with NO and O_3 also significantly changes the OH production rate. These three main pathways are influenced by different factors that are related to different halogen species. SSA and inorganic iodine gases have the most significant impacts on P_{OH}. Both decrease P_{OH} through physical processes including the extinction effect of SSA and the enhancement of ozone deposition by oceanic iodine, while generally increase P_{OH} through chemical processes among which the Cl (from SSA) and inorganic iodine chemistry are the most important. In the continent, SSA is the controlling species and its extinction effect leads to the negative ΔP_{OH} in the southern China. While in the ocean atmosphere, the controlling species are inorganic iodine gases and the complicated iodine chemistry determines the basic pattern of ΔP_{OH}.

Although the uncertainties in estimating the emission rates of different halogen species could influence on the magnitude and even the distribution of the halogen-induced change of P_{OH}, the significant impact of the marine-emitted halogen species on the oceanic OH radical and the potential impact on the coastal atmosphere oxidation in the episodic events have been clearly revealed. In addition, the response of the main contributors of P_{OH} to the individual species and pathway and their influencing factors have been identified, which explains the halogen-induced change of P_{OH} East Asia and also can be applied in other circumstances (e.g., different domains, regions, and emission rates).

https://doi.org/10.5194/acp-2021-876
Preprint. Discussion started: 20 November 2021

Atmospheric Chemistry and Physics Discussions

Data availability

Hourly O_3 concentration data could be obtained from https://quotsoft.net/air/ (Ministry of Environmental Protection of China). NCEP datasets are available at https://rda.ucar.edu. The chl-*a* data can be downloaded from the merged products of the GlobColour data set (http://globcolour.info).

Author contribution

YL designed the study and wrote the manuscript. SF run the simulations, conducted analyses, and wrote the manuscript.

Competing interests

The authors declare that they have no conflict of interest.

Acknowledgment

This work was supported by the National Natural Science Foundation of China (Grant no. 41961160728), the Guangdong Province Science and Technology Planning Project of China (Grant no. 2017A050506003), National Natural Science Foundation of China (Grant no. 41575106), Shenzhen Science and Technology Program (KQTD20180411143441009), Key Special Project for Introduced Talents Team of Southern Marine Science and Engineering Guangdong Laboratory (Guangzhou) (GML2019ZD0210), Guangdong Basic and Applied Basic Research Fund Committee (2020B1515130003)，Key-Area Research and Development Program of Guangdong Province (2020B1111360001), Shenzhen Key Laboratory Foundation (ZDSYS20180208184349083), Center for Computational Science and Engineering at Southern University of Science and Technology.

References

Appel, K. W., Bash, J. O., Fahey, K. M., Foley, K. M., Gilliam, R. C., Hogrefe, C., Hutzell, W. T., Kang, D. W., Mathur, R., Murphy, B. N., Napelenok, S. L., Nolte, C. G., Pleim, J. E., Pouliot, G. A., Pye, H. O. T., Ran, L. M., Roselle, S. J., Sarwar, G., Schwede, D. B., Sidi, F. I., Spero, T. L., and Wong, D. C.: The Community Multiscale Air Quality (CMAQ) model versions 5.3 and 5.3.1: system updates and evaluation, Geoscientific Model Development, 14, 2867-2897, 10.5194/gmd-14-2867-2021, 2021.

Archibald, A. T., Cooke, M. C., Utembe, S. R., Shallcross, D. E., Derwent, R. G., and Jenkin, M. E.: Impacts of mechanistic changes on HOx formation and recycling in the oxidation of isoprene, Atmospheric Chemistry and Physics, 10, 8097-8118, 10.5194/acp-10-8097-2010, 2010.

Barthel, S., Tegen, I., and Wolke, R.: Do new sea spray aerosol source functions improve the results of a regional aerosol model?, Atmospheric Environment, 198, 265-278, 10.1016/j.atmosenv.2018.10.016, 2019.

Bates, K. H., and Jacob, D. J.: A new model mechanism for atmospheric oxidation of isoprene: global effects on oxidants, nitrogen oxides, organic products, and secondary organic aerosol, Atmospheric Chemistry and Physics, 19, 9613-9640, 10.5194/acp-19-9613-2019, 2019.

Carpenter, L. J., MacDonald, S. M., Shaw, M. D., Kumar, R., Saunders, R. W., Parthipan, R., Wilson, J., and Plane, J. M. C.: Atmospheric iodine levels influenced by sea surface emissions of inorganic iodine, Nature Geoscience, 6, 108-111, 10.1038/ngeo1687, 2013.

https://doi.org/10.5194/acp-2021-876
Preprint. Discussion started: 20 November 2021

Atmospheric Chemistry and Physics Discussions

Chance, R., Baker, A. R., Carpenter, L., and Jickells, T. D.: The distribution of iodide at the sea surface, Environmental Science-Processes & Impacts, 16, 1841-1859, 10.1039/c4em00139g, 2014.

Chang, W. N., Heikes, B. G., and Lee, M. H.: Ozone deposition to the sea surface: chemical enhancement and wind speed dependence, Atmospheric Environment, 38, 1053-1059, 10.1016/j.atmosenv.2003.10.050, 2004.

Dai, J. N., Liu, Y. M., Wang, P., Fu, X., Xia, M., and Wang, T.: The impact of sea-salt chloride on ozone through heterogeneous reaction with N_2O_5 in a coastal region of south China, Atmospheric Environment, 236, 10.1016/j.atmosenv.2020.117604, 2020.

Emery, C., Liu, Z., Russell, A. G., Odman, M. T., Yarwood, G., and Kumar, N.: Recommendations on statistics and benchmarks to assess photochemical model performance, Journal of the Air & Waste Management Association, 67, 582-598, 10.1080/10962247.2016.1265027, 2017.

Engel, A., Rigby, M., Burkholder, J., Fernandez, R., Froidevaux, L., Hall, B., Hossaini, R., Saito, T., Vollmer, M., and Yao, B. J. S. A. o. O. D.: Update on Ozone-Depleting Substances (ODSs) and Other Gases of Interest to the Montreal Protocol, in: Scientific Assessment of Ozone Depletion: 2018, 1-87, 2019.

Fairall, C. W., Helmig, D., Ganzeveld, L., and Hare, J.: Water-side turbulence enhancement of ozone deposition to the ocean, Atmospheric Chemistry and Physics, 7, 443-451, 10.5194/acp-7-443-2007, 2007.

Fittschen, C., Al Ajami, M., Batut, S., Ferracci, V., Archer-Nicholls, S., Archibald, A. T., and Schoemaecker, C.: ROOOH: a missing piece of the puzzle for OH measurements in low-NO environments?, Atmospheric Chemistry and Physics, 19, 349-362, 10.5194/acp-19-349-2019, 2019.

Fuchs, H., Hofzumahaus, A., Rohrer, F., Bohn, B., Brauers, T., Dorn, H. P., Haseler, R., Holland, F., Kaminski, M., Li, X., Lu, K., Nehr, S., Tillmann, R., Wegener, R., and Wahner, A.: Experimental evidence for efficient hydroxyl radical regeneration in isoprene oxidation, Nature Geoscience, 6, 1023-1026, 10.1038/ngeo1964, 2013.

Gantt, B., Kelly, J. T., and Bash, J. O.: Updating sea spray aerosol emissions in the Community Multiscale Air Quality (CMAQ) model version 5.0.2, Geoscientific Model Development, 8, 3733-3746, 10.5194/gmd-8-3733-2015, 2015.

Gao, M., Gao, J. H., Zhu, B., Kumar, R., Lu, X., Song, S. J., Zhang, Y. Z., Jia, B. X., Wang, P., Beig, G. R., Hu, J. L., Ying, Q., Zhang, H. L., Sherman, P., and McElroy, M. B.: Ozone pollution over China and India: seasonality and sources, Atmospheric Chemistry and Physics, 20, 4399-4414, 10.5194/acp-20-4399-2020, 2020.

Gong, S. L.: A parameterization of sea-salt aerosol source function for sub- and super-micron particles, Global Biogeochemical Cycles, 17, 10.1029/2003gb002079, 2003.

Grossmann, K., Friess, U., Peters, E., Wittrock, F., Lampel, J., Yilmaz, S., Tschritter, J., Sommariva, R., von Glasow, R., Quack, B., Kruger, K., Pfeilsticker, K., and Platt, U.: Iodine monoxide in the Western Pacific marine boundary layer, Atmospheric Chemistry and Physics, 13, 3363-3378, 10.5194/acp-13-3363-2013, 2013.

Grythe, H., Strom, J., Krejci, R., Quinn, P., and Stohl, A.: A review of sea-spray aerosol source functions using a large global set of sea salt aerosol concentration measurements, Atmospheric Chemistry and Physics, 14, 1277-1297, 10.5194/acp-14-1277-2014, 2014.

Guenther, A. B., Jiang, X., Heald, C. L., Sakulyanontvittaya, T., Duhl, T., Emmons, L. K., and Wang, X.: The Model of Emissions of Gases and Aerosols from Nature version 2.1 (MEGAN2.1): an extended and updated framework for modeling biogenic emissions, Geoscientific Model Development, 5, 1471-1492, 10.5194/gmd-5-1471-2012, 2012.

Hofzumahaus, A., Rohrer, F., Lu, K. D., Bohn, B., Brauers, T., Chang, C. C., Fuchs, H., Holland, F., Kita, K., Kondo, Y., Li, X., Lou, S. R., Shao, M., Zeng, L. M., Wahner, A., and Zhang, Y. H.: Amplified Trace Gas Removal in the Troposphere, Science, 324, 1702-1704, 10.1126/science.1164566, 2009.

Hu, L., Jacob, D. J., Liu, X., Zhang, Y., Zhang, L., Kim, P. S., Sulprizio, M. P., and Yantosca, R. M.: Global budget of tropospheric ozone: Evaluating recent model advances with satellite (OMI), aircraft (IAGOS), and ozonesonde observations, Atmospheric Environment, 167, 323-334, 10.1016/j.atmosenv.2017.08.036, 2017.

Jaeglé, L., Quinn, P. K., Bates, T. S., Alexander, B., and Lin, J. T.: Global distribution of sea salt aerosols: new constraints from in situ and remote sensing observations, Atmospheric Chemistry and Physics, 11, 3137-3157, 10.5194/acp-11-3137-2011, 2011.

Kelly, J. T., Bhave, P. V., Nolte, C. G., Shankar, U., and Foley, K. M.: Simulating emission and chemical evolution of coarse sea-salt particles in the Community Multiscale Air Quality (CMAQ) model, Geoscientific Model Development, 3, 257-273, 10.5194/gmd-3-257-2010, 2010.

Koenig, T. K., Volkamer, R., Baidar, S., Dix, B., Wang, S. Y., Anderson, D. C., Salawitch, R. J., Wales, P. A., Cuevas, C. A., Fernandez, R. P., Saiz-Lopez, A., Evans, M. J., Sherwen, T., Jacob, D. J., Schmidt, J., Kinnison, D., Lamarque, J. F., Apel, E. C., Bresch, J. C., Campos, T., Flocke, F. M., Hall, S. R., Honomichl, S. B., Hornbrook, R., Jensen, J. B., Lueb, R., Montzka, D. D., Pan, L. L., Reeves, J. M., Schauffler, S. M., Ullmann, K., Weinheimer, A. J., Atlas, E. L., Donets, V., Navarro, M. A., Riemer, D., Blake, N. J., Chen, D. X., Huey, L. G., Tanner, D. J., Hanisco, T. F., and Wolfe, G. M.: BrO and inferred Br-y profiles over the western Pacific: relevance of inorganic bromine sources and a Br-y minimum in the aged tropical tropopause layer, Atmospheric Chemistry and Physics, 17, 15245-15270, 10.5194/acp-17-15245-2017, 2017.

Le Breton, M., Bannan, T. J., Shallcross, D. E., Khan, M. A., Evans, M. J., Lee, J., Lidster, R., Andrews, S., Carpenter, L. J., Schmidt, J., Jacob, D., Harris, N. R. P., Bauguitte, S., Gallagher, M., Bacak, A., Leather, K. E., and Percival, C. J.: Enhanced ozone loss by

https://doi.org/10.5194/acp-2021-876
Preprint. Discussion started: 20 November 2021

active inorganic bromine chemistry in the tropical troposphere, Atmospheric Environment, 155, 21-28, 10.1016/j.atmosenv.2017.02.003, 2017.

Lelieveld, J., Butler, T. M., Crowley, J. N., Dillon, T. J., Fischer, H., Ganzeveld, L., Harder, H., Lawrence, M. G., Martinez, M., Taraborrelli, D., and Williams, J.: Atmospheric oxidation capacity sustained by a tropical forest, Nature, 452, 737-740, 10.1038/nature06870, 2008.

Li, Q. Y., Borge, R., Sarwar, G., de la Paz, D., Gantt, B., Domingo, J., Cuevas, C. A., and Saiz-Lopez, A.: Impact of halogen chemistry on summertime air quality in coastal and continental Europe: application of the CMAQ model and implications for regulation, Atmospheric Chemistry and Physics, 19, 15321-15337, 10.5194/acp-19-15321-2019, 2019.

Li, Q. Y., Badia, A., Wang, T., Sarwar, G., Fu, X., Zhang, L., Zhang, Q., Fung, J., Cuevas, C. A., Wang, S. S., Zhou, B., and Saiz-Lopez, A.: Potential Effect of Halogens on Atmospheric Oxidation and Air Quality in China, Journal of Geophysical Research: Atmospheres, 125, 10.1029/2019jd032058, 2020.

Liu, S., Liu, C.-C., Froyd, K. D., Schill, G. P., Murphy, D. M., Bui, T. P., Dean-Day, J. M., Weinzierl, B., Dollner, M., Diskin, G. S., Chen, G., and Gao, R.-S.: Sea spray aerosol concentration modulated by sea surface temperature, Proceedings of the National Academy of Sciences, 118, e2020583118, 10.1073/pnas.2020583118, 2021.

Liu, Y. L., Nie, W., Xu, Z., Wang, T. Y., Wang, R. X., Li, Y. Y., Wang, L., Chi, X. G., and Ding, A. J.: Semi-quantitative understanding of source contribution to nitrous acid (HONO) based on 1 year of continuous observation at the SORPES station in eastern China, Atmospheric Chemistry and Physics, 19, 13289-13308, 10.5194/acp-19-13289-2019, 2019.

Loades, D. C., Yang, M. X., Belli, T. G., Vaughan, A. R., Pound, R. J., Metzger, S., Lee, J. D., and Carpenter, L. J.: Ozone deposition to a coastal sea: comparison of eddy covariance observations with reactive air-sea exchange models, Atmospheric Measurement Techniques, 13, 6915-6931, 10.5194/amt-13-6915-2020, 2020.

Lu, K. D., Guo, S., Tan, Z. F., Wang, H. C., Shang, D. J., Liu, Y. H., Li, X., Wu, Z. J., Hu, M., and Zhang, Y. H.: Exploring atmospheric free-radical chemistry in China: the self-cleansing capacity and the formation of secondary air pollution, National Science Review, 6, 579-594, 10.1093/nsr/nwy073, 2019a.

Lu, X., Zhang, L., Chen, Y., Zhou, M., Zheng, B., Li, K., Liu, Y., Lin, J., Fu, T. M., and Zhang, Q.: Exploring 2016–2017 surface ozone pollution over China: source contributions and meteorological influences, Atmospheric Chemistry and Physics, 19, 8339-8361, 10.5194/acp-19-8339-2019, 2019b.

Luhar, A. K., Galbally, I. E., Woodhouse, M. T., and Thatcher, M.: An improved parameterisation of ozone dry deposition to the ocean and its impact in a global climate-chemistry model, Atmospheric Chemistry and Physics, 17, 3749-3767, 10.5194/acp-17-3749-2017, 2017.

Luhar, A. K., Woodhouse, M. T., and Galbally, I. E.: A revised global ozone dry deposition estimate based on a new two-layer parameterisation for air-sea exchange and the multi-year MACC composition reanalysis, Atmospheric Chemistry and Physics, 18, 4329-4348, 10.5194/acp-18-4329-2018, 2018.

MacDonald, S. M., Martin, J. C. G., Chance, R., Warriner, S., Saiz-Lopez, A., Carpenter, L. J., and Plane, J. M. C.: A laboratory characterisation of inorganic iodine emissions from the sea surface: dependence on oceanic variables and parameterisation for global modelling, Atmospheric Chemistry and Physics, 14, 5841-5852, 10.5194/acp-14-5841-2014, 2014.

Mahajan, A. S., Li, Q., Inamdar, S., Ram, K., Badia, A., and Saiz-Lopez, A.: Modelling the impacts of iodine chemistry on the northern Indian Ocean marine boundary layer, Atmospheric Chemistry and Physics, 21, 8437-8454, 10.5194/acp-21-8437-2021, 2021.

Monahan, E., Spiel, D., and Davidson, K.: A model of marine aerosol generation via whitecaps and wave disruption, in: Oceanic whitecaps, Springer, 167-174, 1986.

Ordonez, C., Lamarque, J. F., Tilmes, S., Kinnison, D. E., Atlas, E. L., Blake, D. R., Santos, G. S., Brasseur, G., and Saiz-Lopez, A.: Bromine and iodine chemistry in a global chemistry-climate model: description and evaluation of very short-lived oceanic sources, Atmospheric Chemistry and Physics, 12, 1423-1447, 10.5194/acp-12-1423-2012, 2012.

Ovadnevaite, J., Manders, A., de Leeuw, G., Ceburnis, D., Monahan, C., Partanen, A. I., Korhonen, H., and O'Dowd, C. D.: A sea spray aerosol flux parameterization encapsulating wave state, Atmospheric Chemistry and Physics, 14, 1837-1852, 10.5194/acp-14-1837-2014, 2014.

Pound, R. J., Sherwen, T., Helmig, D., Carpenter, L. J., and Evans, M. J.: Influences of oceanic ozone deposition on tropospheric photochemistry, Atmospheric Chemistry and Physics, 20, 4227-4239, 10.5194/acp-20-4227-2020, 2020.

Read, K. A., Mahajan, A. S., Carpenter, L. J., Evans, M. J., Faria, B. V. E., Heard, D. E., Hopkins, J. R., Lee, J. D., Moller, S. J., Lewis, A. C., Mendes, L., McQuaid, J. B., Oetjen, H., Saiz-Lopez, A., Pilling, M. J., and Plane, J. M. C.: Extensive halogen-mediated ozone destruction over the tropical Atlantic Ocean, Nature, 453, 1232-1235, 10.1038/nature07035, 2008.

Rohrer, F., Lu, K. D., Hofzumahaus, A., Bohn, B., Brauers, T., Chang, C. C., Fuchs, H., Haseler, R., Holland, F., Hu, M., Kita, K., Kondo, Y., Li, X., Lou, S. R., Oebel, A., Shao, M., Zeng, L. M., Zhu, T., Zhang, Y. H., and Wahner, A.: Maximum efficiency in the hydroxyl-radical-based self-cleansing of the troposphere, Nature Geoscience, 7, 559-563, 10.1038/ngeo2199, 2014.

Saiz-Lopez, A., and von Glasow, R.: Reactive halogen chemistry in the troposphere, Chemical Society Reviews, 41, 6448-6472, 10.1039/c2cs35208g, 2012.

https://doi.org/10.5194/acp-2021-876
Preprint. Discussion started: 20 November 2021

Atmospheric Chemistry and Physics Discussions

Sarwar, G., Gantt, B., Schwede, D., Foley, K., Mathur, R., and Saiz-Lopez, A.: Impact of Enhanced Ozone Deposition and Halogen Chemistry on Tropospheric Ozone over the Northern Hemisphere, Environmental Science & Technology, 49, 9203-9211, 10.1021/acs.est.5b01657, 2015.

Sarwar, G., Gantt, B., Foley, K., Fahey, K., Spero, T. L., Kang, D. W., Mathur, R., Foroutan, H., Xing, J., Sherwen, T., and Saiz-Lopez, A.: Influence of bromine and iodine chemistry on annual, seasonal, diurnal, and background ozone: CMAQ simulations over the Northern Hemisphere, Atmospheric Environment, 213, 395-404, 10.1016/j.atmosenv.2019.06.020, 2019.

Sekiya, T., Kanaya, Y., Sudo, K., Taketani, F., Iwamoto, Y., Aita, M. N., Yamamoto, A., and Kawamoto, K.: Global Bromine- and Iodine-Mediated Tropospheric Ozone Loss Estimated Using the CHASER Chemical Transport Model, Sola, 16, 220-227, 10.2151/sola.2020-037, 2020.

Sherwen, T., Schmidt, J. A., Evans, M. J., Carpenter, L. J., Grossmann, K., Eastham, S. D., Jacob, D. J., Dix, B., Koenig, T. K., Sinreich, R., Ortega, I., Volkamer, R., Saiz-Lopez, A., Prados-Roman, C., Mahajan, A. S., and Ordonez, C.: Global impacts of tropospheric halogens (Cl, Br, I) on oxidants and composition in GEOS-Chem, Atmospheric Chemistry and Physics, 16, 12239-12271, 10.5194/acp-16-12239-2016, 2016.

Sherwen, T., Chance, R. J., Tinel, L., Ellis, D., Evans, M. J., and Carpenter, L. J.: A machine-learning-based global sea-surface iodide distribution, Earth System Science Data, 11, 1239-1262, 10.5194/essd-11-1239-2019, 2019.

Simpson, W. R., Brown, S. S., Saiz-Lopez, A., Thornton, J. A., and von Glasow, R.: Tropospheric Halogen Chemistry: Sources, Cycling, and Impacts, Chemical Reviews, 115, 4035-4062, 10.1021/cr5006638, 2015.

Song, H., Chen, X., Lu, K., Zou, Q., Tan, Z., Fuchs, H., Wiedensohler, A., Moon, D. R., Heard, D. E., Baeza-Romero, M. T., Zheng, M., Wahner, A., Kiendler-Scharr, A., and Zhang, Y.: Influence of aerosol copper on HO_2 uptake: a novel parameterized equation, Atmospheric Chemistry and Physics, 20, 15835-15850, 10.5194/acp-20-15835-2020, 2020.

Stone, D., Whalley, L. K., and Heard, D. E.: Tropospheric OH and HO_2 radicals: field measurements and model comparisons, Chemical Society Reviews, 41, 6348-6404, 10.1039/c2cs35140d, 2012.

Stone, D., Sherwen, T., Evans, M. J., Vaughan, S., Ingham, T., Whalley, L. K., Edwards, P. M., Read, K. A., Lee, J. D., Moller, S. J., Carpenter, L. J., Lewis, A. C., and Heard, D. E.: Impacts of bromine and iodine chemistry on tropospheric OH and HO_2: comparing observations with box and global model perspectives, Atmospheric Chemistry and Physics, 18, 3541-3561, 10.5194/acp-18-3541-2018, 2018.

Tan, Z. F., Lu, K. D., Hofzumahaus, A., Fuchs, H., Bohn, B., Holland, F., Liu, Y. H., Rohrer, F., Shao, M., Sun, K., Wu, Y. S., Zeng, L. M., Zhang, Y. S., Zou, Q., Kiendler-Scharr, A., Wahner, A., and Zhang, Y. H.: Experimental budgets of OH, HO2, and RO2 radicals and implications for ozone formation in the Pearl River Delta in China 2014, Atmospheric Chemistry and Physics, 19, 7129-7150, 10.5194/acp-19-7129-2019, 2019.

Tham, Y. J., He, X.-C., Li, Q., Cuevas, C. A., Shen, J., Kalliokoski, J., Yan, C., Iyer, S., Lehmusjärvi, T., Jang, S., Thakur, R. C., Beck, L., Kemppainen, D., Olin, M., Sarnela, N., Mikkilä, J., Hakala, J., Marbouti, M., Yao, L., Li, H., Huang, W., Wang, Y., Wimmer, D., Zha, Q., Virkanen, J., Spain, T. G., O'Doherty, S., Jokinen, T., Bianchi, F., Petäjä, T., Worsnop, D. R., Mauldin, R. L., Ovadnevaite, J., Ceburnis, D., Maier, N. M., Kulmala, M., O'Dowd, C., Dal Maso, M., Saiz-Lopez, A., and Sipilä, M.: Direct field evidence of autocatalytic iodine release from atmospheric aerosol, Proceedings of the National Academy of Sciences, 118, e2009951118, 10.1073/pnas.2009951118, 2021.

Wang, X., Jacob, D. J., Eastham, S. D., Sulprizio, M. P., Zhu, L., Chen, Q. J., Alexander, B., Sherwen, T., Evans, M. J., Lee, B. H., Haskins, J. D., Lopez-Hilfiker, F. D., Thornton, J. A., Huey, G. L., and Liao, H.: The role of chlorine in global tropospheric chemistry, Atmospheric Chemistry and Physics, 19, 3981-4003, 10.5194/acp-19-3981-2019, 2019.

Wang, X., Jacob, D. J., Fu, X., Wang, T., Le Breton, M., Hallquist, M., Liu, Z. R., McDuffie, E. E., and Liao, H.: Effects of Anthropogenic Chlorine on $PM_{2.5}$ and Ozone Air Quality in China, Environmental Science & Technology, 54, 9908-9916, 10.1021/acs.est.0c02296, 2020.

Wang, X., Jacob, D. J., Downs, W., Zhai, S., Zhu, L., Shah, V., Holmes, C. D., Sherwen, T., Alexander, B., Evans, M. J., Eastham, S. D., Neuman, J. A., Veres, P., Koenig, T. K., Volkamer, R., Huey, L. G., Bannan, T. J., Percival, C. J., Lee, B. H., and Thornton, J. A.: Global tropospheric halogen (Cl, Br, I) chemistry and its impact on oxidants, Atmos. Chem. Phys. Discuss., 2021, 1-34, 10.5194/acp-2021-441, 2021.

Whalley, L. K., Furneaux, K. L., Goddard, A., Lee, J. D., Mahajan, A., Oetjen, H., Read, K. A., Kaaden, N., Carpenter, L. J., Lewis, A. C., Plane, J. M. C., Saltzman, E. S., Wiedensohler, A., and Heard, D. E.: The chemistry of OH and HO_2 radicals in the boundary layer over the tropical Atlantic Ocean, Atmospheric Chemistry and Physics, 10, 1555-1576, 10.5194/acp-10-1555-2010, 2010.

Whalley, L. K., Slater, E. J., Woodward-Massey, R., Ye, C., Lee, J. D., Squires, F., Hopkins, J. R., Dunmore, R. E., Shaw, M., Hamilton, J. F., Lewis, A. C., Mehra, A., Worrall, S. D., Bacak, A., Bannan, T. J., Coe, H., Percival, C. J., Ouyang, B., Jones, R. L., Crilley, L. R., Kramer, L. J., Bloss, W. J., Vu, T., Kotthaus, S., Grimmond, S., Sun, Y., Xu, W., Yue, S., Ren, L., Acton, W. J. F., Hewitt, C. N., Wang, X., Fu, P., and Heard, D. E.: Evaluating the sensitivity of radical chemistry and ozone formation to ambient VOCs and NOx in Beijing, Atmospheric Chemistry and Physics, 21, 2125-2147, 10.5194/acp-21-2125-2021, 2021.

https://doi.org/10.5194/acp-2021-876
Preprint. Discussion started: 20 November 2021

Atmospheric Chemistry and Physics Discussions

Yin, S. S., Zheng, J. Y., Lu, Q., Yuan, Z. B., Huang, Z. J., Zhong, L. J., and Lin, H.: A refined 2010-based VOC emission inventory and its improvement on modeling regional ozone in the Pearl River Delta Region, China, Science of the Total Environment, 514, 426-438, 10.1016/j.scitotenv.2015.01.088, 2015.

Yu, C., Wang, Z., Xia, M., Fu, X., Wang, W., Tham, Y. J., Chen, T., Zheng, P., Li, H., Shan, Y., Wang, X., Xue, L., Zhou, Y., Yue, D., Ou, Y., Gao, J., Lu, K., Brown, S. S., Zhang, Y., and Wang, T.: Heterogeneous N_2O_5 reactions on atmospheric aerosols at four Chinese sites: improving model representation of uptake parameters, Atmospheric Chemistry and Physics, 20, 4367-4378, 10.5194/acp-20-4367-2020, 2020.

Zheng, J. Y., Zhang, L. J., Che, W. W., Zheng, Z. Y., and Yin, S. S.: A highly resolved temporal and spatial air pollutant emission inventory for the Pearl River Delta region, China and its uncertainty assessment, Atmospheric Environment, 43, 5112-5122, 10.1016/j.atmosenv.2009.04.060, 2009.

Zhou, J., Murano, K., Kohno, N., Sakamoto, Y., and Kajii, Y.: Real-time quantification of the total HO2 reactivity of ambient air and HO2 uptake kinetics onto ambient aerosols in Kyoto (Japan), Atmospheric Environment, 223, 10.1016/j.atmosenv.2020.117189, 2020.

Zhou, J., Sato, K., Bai, Y., Fukusaki, Y., Kousa, Y., Ramasamy, S., Takami, A., Yoshino, A., Nakayama, T., Sadanaga, Y., Nakashima, Y., Li, J., Murano, K., Kohno, N., Sakamoto, Y., and Kajii, Y.: Kinetics and impacting factors of HO_2 uptake onto submicron atmospheric aerosols during the 2019 Air QUAlity Study (AQUAS) in Yokohama, Japan, Atmospheric Chemistry and Physics, 21, 12243-12260, 10.5194/acp-21-12243-2021, 2021.

Zhu, L., Jacob, D. J., Eastham, S. D., Sulprizio, M. P., Wang, X., Sherwen, T., Evans, M. J., Chen, Q. J., Alexander, B., Koenig, T. K., Volkamer, R., Huey, L. G., Le Breton, M., Bannan, T. J., and Percival, C. J.: Effect of sea salt aerosol on tropospheric bromine chemistry, Atmospheric Chemistry and Physics, 19, 6497-6507, 10.5194/acp-19-6497-2019, 2019.